Numerical Computation of the EM Coupling Between a Circular Loop Antenna and a Full-Scale Human-Body Model

W.-T. Chen and H.-R. Chuang

***Abstract*—This paper presents numerical computation of the electromagnetic (EM) coupling between circular loop antennas and a full-scale human-body model. The loop antenna can be x-, y-, or z-oriented. Coupled integral equations (CIE's) and the method of moments (MoM) are employed to numerically solve this antenna–body-coupling problem. Numerical results of the antenna radiation characteristics influenced by the human body and the body-absorption rate from 50 to 400 MHz are presented. The applications of this study include assessment of a radio-frequency (RF) dose from a loop antenna and the body effect on the performance of the loop antenna used in personal communication devices such as radio pagers.**

***Index Terms*—EM coupling, human body, loop antenna, RF dose.**

I. Introduction

Recently, there has been much research studying the electromagnetic (EM) interaction between the dipole-type antenna and the human body for portable/personal communication interests and radio-frequency (RF) safety issues [1]–[3]. However, the EM coupling effect between the loop antenna and a realistically shaped full-scale human-body model has yet to be further investigated. The interests include the body absorption of the radiated power from the proximate loop radiator for RF dose assessment and the communication performance of the radio-pager's internal loop antenna affected by the human operator within vicinity [4]. In [5], the human body was replaced as a large conducting reflector plane, and the image theory was applied to analyze this loop antenna and body coupling problem. The body-absorption effect is not included in this crude analysis. In [6], a human-head model was employed to numerically study the coupling effects on the loop antenna. In many cases, such as the loop antenna of the radio pager kept very close to the abdomen of the human operator, a realistically shaped full-scale human-body model is necessary for full investigation.

In this paper, a circular loop antenna and a full-scale human-body model are used to study the body effect on the loop-antenna characteristics and the body-absorption rate. Coupled integral equations (CIE's) and the method of moments (MoM) are used to analyze this EM coupling problem [7]. Both the Galerkin and point-matching techniques are applied in the MoM procedure. Numerical results of the loop with x-, y-, and z- orientations in free space, and proximate to the body from 50–400 MHz, are presented. The loop-antenna radiation characteristics at a 280-MHz very high frequency (VHF) radio-paging band affected by the body is studied. The rate of the power absorbed by the human body from 50 to 400 MHz is also calculated for the RF dose assessment.

II. Theoretical Analysis

Fig. 1 illustrates a circular loop wire antenna located close to a human body. The orientation of the loop antenna is defined by the vector, which is normal to the loop plane. The loop with x-, y-, and z- orientations are considered. The loop antenna is excited by a delta–gap generator of driving-point input voltage V_o. The loop radius is b and the wire radius is a. The electric parameters of the human-body tissue are expressed as (σ, ε, μ_0) and are assumed to be a nonmagnetic medium. By using the dyadic Green's function technique, the integral equation for the electric field induced inside the body from the nearby radiating antenna and the antenna current distribution along the surface of the perfectly conducting wire antenna are given as (1)–(3), shown at the bottom of the following page, where V_b is the volume of the body and $\hat{s}$ (or $\hat{s}'$) is the unit tangential vector of the field (or source) point on the antenna surface [7]–[13]. Equations (1) and (2) are solved numerically by the MoM. The loop-antenna current is expanded by the piecewise sinusoidal basis functions. The electric field in the body is expressed by the pulse basis functions. In the MoM procedure, the point-matching technique is applied to (1) and the Galerkin technique is applied to (2).

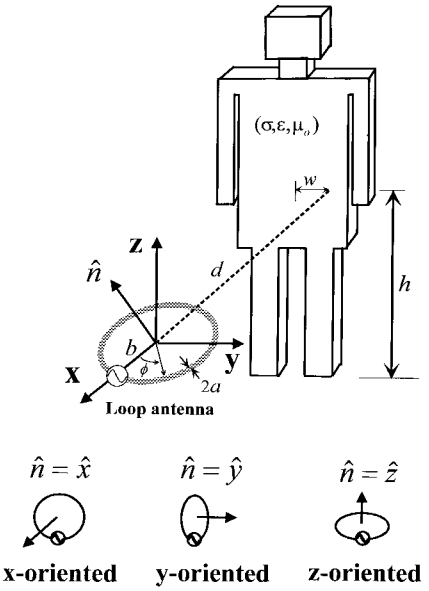

Fig. 1. A circular loop antenna proximate to a human body.

The total radiation field ($\vec{E}^r$, $\vec{H}^r$) is the sum of the radiation field from the antenna and the scattered field from the body. The radiation power to free space, body absorbed power, and antenna directive gain G can be expressed as

$$P_{\rm rad} = \oint_s \frac{1}{2}\,{\rm Re}[\vec{E}^r \times \vec{H}^{r^*}] \cdot d\vec{s}$$

$$P_{\rm abs} = \int_{V_b} \frac{1}{2}\,\sigma|\vec{E}|^2\,dv$$

$$G(\theta,\phi) = \frac{1/2\ {\rm Re}[\vec{E}^r \times \vec{H}^{r^*}]}{P_{\rm rad}/(4\pi r^2)}. \tag{4}$$

Under the perfect-conductor assumption for the loop wire, the antenna input impedance Z_i and the real power delivered to the antenna (for radiation) is given by

$$Z_i = V_o/I_o \quad P_{\rm in\_PEC} = \tfrac{1}{2}\,{\rm Re}(V_o I_o^*) \tag{5}$$

where I_0 is the antenna current at the feed point. Since the power delivered to the antenna should be equal to the sum of the body-

Manuscript received January 23, 1997; revised November 21, 1997. This work was supported in part by the National Science Council, R.O.C., under Grant NCHC-86-03-011 and under Grant NSC 87-2218-E-006-058.

The authors are with the Department of Electrical Engineering, National Cheng Kung University, 70101 Tainan, Taiwan, R.O.C.

Publisher Item Identifier S 0018-9480(98)07230-5.

absorbed power $P_{\rm abs}$ and the radiation power (to free space) $P_{\rm rad}$, these quantities can be used to check the EM coupling computation accuracy. The computation error is defined as

$$\text{computation error} = |P_{\rm in\_PEC} - (P_{\rm rad} + P_{\rm abs})|/P_{\rm in\_PEC}. \quad (6)$$

In practice, since the conductivity σ_c of the loop wire is finite, an ohmic-loss resistance exists. For an electrically small loop antenna, the ohmic-loss resistance is given by [14], and the ohmic-loss radiation efficiency can be defined by

$$R_{\rm ohm} = \sqrt{\pi f \mu_0/\sigma_c}\,(b/a) \quad \eta_{r\Omega} = R_r/(R_r + R_{\rm ohm}) \quad (7)$$

where R_r represents the radiation resistance (real part of the input impedance). Also, due to the human-body absorption, the body-absorption radiation efficiency η_{rb} is defined by

$$\eta_{rb} = P_{\rm rad}/(P_{\rm rad} + P_{\rm abs}) = P_{\rm rad}/P_{\rm radl}$$
$$P_{\rm radl} = P_{\rm rad} + P_{\rm abs} = \text{the radiation power leaving the antenna.} \quad (8)$$

The antenna power gain is then expressed as

$$G_p = \eta_{r\Omega}\eta_{rb}G. \quad (9)$$

It is important that the power gain defined under the body absorption should be used to evaluate the antenna performance in the communication-link budget.

Although, in this analysis, the loop antenna is treated as a transmitting antenna, the computed radiation characteristics can also be used for a receiving antenna from the reciprocity point of view (if the human body is an EM linear system). It is also important to note that for the receiving-system analysis [such as signal-to-noise ratio (SNR)] the antenna noise T_A can be expressed as [14]

$$T_A = \eta_{r\Omega}T_b + (1 - \eta_{r\Omega})T_P \quad (10)$$

where T_b is the background noise temperature and T_P is the antenna physical temperature, and only the ohmic-loss radiation efficiency $\eta_{r\Omega}$ is related. The two different radiation efficiencies should be used carefully in the receiving-system analysis.

III. Numerical Results

A realistically shaped human model with a height of 170 cm is constructed. Since the main interest is the body effect on the antenna radiation characteristics, the human body is modeled as a homogeneous muscle phantom with relative permittivity constant ε_r and conductivity σ, shown in Table I [15]. The loop antenna is located adjacent to the center of the abdomen ($d = 2$ cm, $w = 0$ cm, $h = 100$ cm) with loop radius $b = 1.7$ cm and wire radius $a = 0.072$ cm ($kb = 0.1$ at 280 MHz). For MoM numerical computation, the loop is divided to 60 segments and the body is partitioned to 280 cubic cells with a cell size of 5 cm. The three-dimensional (3-D) Gaussian quadrature method with six points in each dimension is employed for the numerical volume integrals in the CIE's.

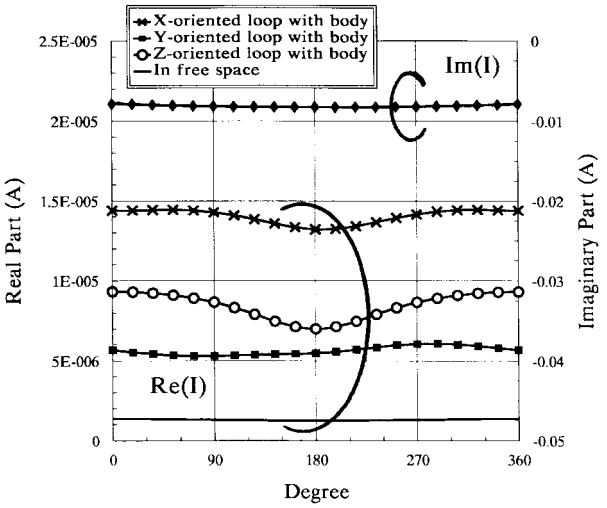

	Input Impedance	Ohmic-loss Efficiency $\eta_{r\Omega}$ (%)
loop in free space	0.022+j129	18
x-oriented loop (close to body)	0.240+j129	70
y-oriented loop (close to body)	0.094+j129	48
z-oriented loop (close to body)	0.155+j129	60

Fig. 2. 280-MHz numerical results of the current distribution and input impedance of the x-, y-, and z-oriented loop antenna located adjacent to the center of the human abdomen ($d = 2$ cm, $w = 0$ cm, $h = 100$ cm). Loop radius $b = 1.7$ cm ($kb = 0.1$ at 280 MHz). Wire radius $a = 0.072$ cm (Hallen factor $2\ln(2\pi b/a) = 10$). Loop-wire ohmic-loss resistance $R_{\rm ohm} = 0.103\ \Omega$ for copper ($\sigma_c = 5.8 \times 10^7$ S/m) at 280 MHz.

Fig. 2 shows numerical results of the current distribution and input impedance of the x-, y-, and z-oriented loop antennas located adjacent to the center of the human abdomen and in free space at 280 MHz (VHF radio-paging band). The imaginary part of the current has almost no change, and the real part of that is highly enhanced when close to the body. It is observed that the real part of the input current of the x-, y-, and z-oriented loop increases approximately ten, four, and six times, respectively. This corresponds to the enhancement of the real part of the antenna input impedance (also shown in Fig. 2) by the human body approximately ten times (x-oriented loop), four times (y-oriented loop), and six times (z-oriented loop), respectively. The imaginary part of the antenna input impedance has almost no

$$\left[1 + \frac{\tau(\vec{r})}{3j\omega\varepsilon_o}\right]\vec{E}(\vec{r}) - PV\int_{V_b}\tau(\vec{\tau}')\vec{E}(\vec{r}')\cdot\vec{\vec{G}}(\vec{r},\vec{r}')\,dv'$$
$$= \int_{\rm ant} I(s')\hat{s}'\cdot\vec{\vec{G}}(\vec{r},s')\,ds' \quad (1)$$

$$\frac{1}{j\omega\varepsilon_o}\int_{\rm ant}\left[\hat{s}\cdot\hat{s}'k_o^2 I(s') + \frac{\partial I(s')}{\partial s'}\frac{\partial}{\partial s}\right]G(s,s')\,ds' + \int_{V_b}\hat{s}\cdot\vec{\vec{G}}(s,\vec{r}')\cdot\tau(\vec{r}')\vec{E}(\vec{r}')\,dv'$$
$$= -V_o\delta(s) \quad (2)$$

$$\tau(\vec{r}) = \sigma(\vec{r}) + j\omega[\varepsilon(\vec{r}) - \varepsilon_o]$$
$$\tilde{G}(\vec{r},\vec{r}') = -j\omega\mu_o\left[\vec{\vec{I}} + \frac{1}{k_o^2}\nabla\nabla\right]G(\vec{r},\vec{r}')$$
$$G(\vec{r},\vec{r}') = e^{-jk_0|\vec{r}-\vec{r}'|}/4\pi|\vec{r}-\vec{r}'| \quad (3)$$

TABLE I
NUMERICAL RESULTS OF THE RADIATION CHARACTERISTICS OF A Y-ORIENTED LOOP ANTENNA IN FREE SPACE OR ADJACENT TO THE CENTER OF THE HUMAN ABDOMEN ($d = 2$ cm, $w = 0$ cm, $h = 100$ cm) FROM 50 TO 400 MHz. LOOP RADIUS $b = 1.7$ cm ($kb = 0.1$ AT 280 MHz). WIRE RADIUS $a = 0.072$ cm (HALLEN FACTOR $\Omega = 2\ln(2\pi b/a) = 10$)

Frequency (MHz)	50	100	200	280	400
Human Muscle Tissue (ε_r, σ)	(92.1, 0.71)	(71.7, 0.89)	(56.5, 1.28)	(54.5, 1.35)	(53.2, 1.41)
Ohmic-loss Resistance (Ω)	0.043	0.061	0.088	0.103	0.125
Input Impedance in Free Space (Ω)	$5.0\text{x}10^{-5}$+j23	$3.1\text{x}10^{-4}$+j45	0.006+j90	0.022+j129	0.11+j196
Ohmic-loss Efficiency $\eta_{r\Omega}$ (%)	0.12	0.51	6.4	17.6	46.8
Noise Temperature** T_A (K)	299	299	293.6	282.4	253.2
Input Impedance proximate to Human Body (Ω)	$2.9\text{x}10^{-4}$+j23	$9.5\text{x}10^{-4}$+j45	0.035+j90	0.094+j129	0.26+j196
Ohmic-loss Efficiency $\eta_{r\Omega}$ (%)	0.67	13.4	28.8	48	67.5
Body-absorption Efficiency η_{rb} (%)	28.1	47.9	40.9	60	67
Total Radiation Efficiency* η_{rt} (%)	0.19	6.4	11.8	28.8	45.2
Noise Temperature** T_A (K)	299.3	286.6	271.2	252	232.5
Computation Error (%)	1.3	0.35	0.27	0.8	2.4

280 MHz	In free space	proximate to human body
E_θ H-plane Max. Directive Gain (dB)	1.52	-3.91
E_θ H-plane Min Directive. Gain (dB)	<-100	-9.07
E_ϕ H-plane Max. Directive Gain (dB)	-12.4	-15.9
E_ϕ H-plane Min. Directive Gain (dB)	<-100	<-100
E_θ H-plane Max. Power Gain (dB)	-5.93	-1.49
E_θ H-plane Min. Power Gain (dB)	<-100	-14.47
E_ϕ H-plane Max. Power Gain (dB)	-19.9	-21.3
E_ϕ H-plane Min. Power Gain (dB)	<-100	<-100

* Total Radiation Efficiency $\eta_{rt} = \eta_{r\Omega} \times \eta_{rb}$
** Assuming T_b=200 K and T_p=300 K

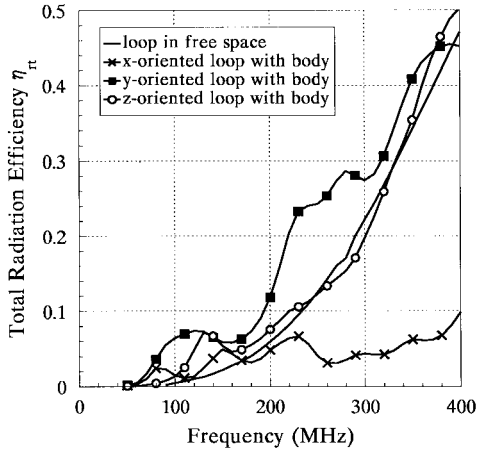

Fig. 3. Computed antenna radiation efficiency versus frequency for loop antennas located adjacent to the center of the human abdomen ($d = 2$ cm, $w = 0$ cm, $h = 100$ cm). Loop radius $b = 1.7$ cm ($k_b = 0.1$ at 280 MHz). Wire radius $a = 0.072$ cm (Hallen factor $2\ln(2\pi b/a) = 10$).

change. By considering the antenna ohmic-loss resistance [copper $\sigma_c = 5.8 \times 10^7$ S/m], the ohmic-loss efficiency $\eta_{r\Omega}$ for the x-, y-, and z-oriented loop antennas close to the body and in free space at 280 MHz are 70%, 48%, 60%, and 18%, respectively (see Fig. 2). The increase of radiation resistance indicates a positive effect of the body, which enhances $\eta_{r\Omega}$.

Fig. 3 shows the total antenna efficiency η_{rt}, which is the product of the body-absorption efficiency and the ohmic-loss efficiency $\eta_{r\Omega}$ versus frequency (see Table I). The dielectric constant ε_r and conductivity σ of the muscle tissue from 50 to 400 MHz are listed in Table I [15]. It is observed that ε_r becomes lower at higher frequency and, on the contrary, for σ. Overall, the x-oriented loop has the lowest efficiency (less than 10%). This is because the main radiating direction of the x-oriented loop is toward the human body. In general, the y-oriented loop antenna has the highest total antenna efficiency. This is the reason that the vertically polarized y-oriented loop antenna is used in a radio pager (see Fig. 4). Note that for the loop antenna in free space, although η_{rb} is equal to one (no body absorption), the ohmic-loss efficiency is very low and, hence, its total efficiency is less than the y-oriented loop proximate to the body. It is also observed that the total efficiency increases with frequency.

Fig. 4 presents the two-dimensional (2-D) power gain patterns of the E_θ (vertical polarization) and E_ϕ (horizontal polarization) fields of the x-, y-, and z-oriented loop antennas in the H-plane ($\theta = 90^\circ$) at 280 MHz for VHF radio-paging application. The two radiation efficiencies η_{rb} and $\eta_{r\Omega}$ were taken into account to compute the power gain patterns [see (9)]. It can be seen that the coupling and absorption effects of the nearby human body significantly affect the radiation patterns. For the x-oriented loop antenna, the E_θ power pattern is highly attenuated for up to 10 dB. This is because a large part (up to 95%) of the power radiated from the antenna is absorbed by the body, although the radiation efficiencies $\eta_{r\Omega}$ are enhanced by the body. However, the body coupling effect enhances the E_ϕ power pattern for approximately 8 dB in the backward direction ($\phi = 180^\circ$). For the y-oriented loop antenna, the two nulls in 90° and 270° directions of the free-space E_θ pattern are "filled" when the loop antenna is close to the body. This is a positive effect of the body coupling, which enhances the power gain in the two null directions for the desired omnidirectional pattern in radio-paging communication. The expected attenuation of the E_θ field toward the direction of the body ($\phi = 180^\circ$) is observed, and the maximum attenuation level is about 10 dB. However, the enhancement of the power gain in the front direction of the body is approximately 4 dB. For the z-oriented loop antenna in the H-plane, there is almost no E_θ field, and the E_ϕ field is enhanced approximately 3 dB in the front direction, and is attenuated approximately 3 dB in the backward direction. Numerical data of the maximum and minimum directive/power gains of the y-oriented loop antenna are shown in Table I. Fig. 5 shows the three kinds of radiation efficiency of the y-oriented loop as a function of the lateral distance w from the center of the abdomen (see Fig. 1). It

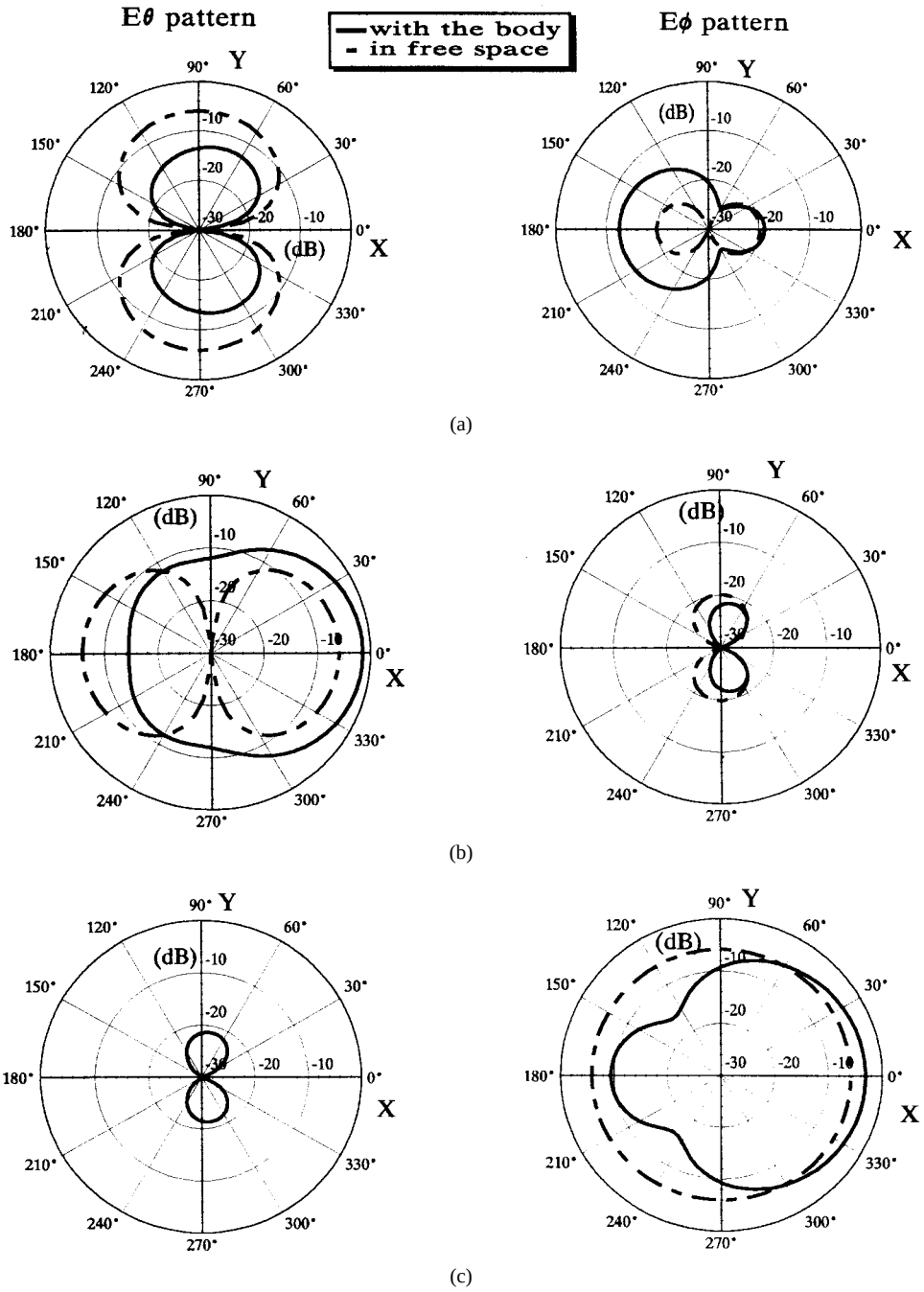

Fig. 4. Computed power patterns ($G_p = \eta_{r\Omega}\eta_{rb}G$) of E_θ and E_ϕ fields in the H-plane for loop antennas in free space or adjacent to the center of the human abdomen ($d = 2$ cm, $w = 0$ cm, $h = 100$ cm). (a) x-oriented loop. (b) y-oriented loop. (c) z-oriented loop. Loop radius $b = 1.7$ cm ($kb = 0.1$ at 280 MHz). Wire radius $a = 0.072$ cm (Hallen factor $2\ln(2\pi b/a) = 10$).

is observed that the variation of the total radiation efficiency versus the lateral distance w is not high.

Table I summarizes radiation characteristics and body absorption of a y-oriented loop antenna in free space, which is adjacent to the center of the human abdomen from 50 to 400 MHz. It is observed that the increasing rate of the real part of the antenna input impedance (radiation resistance) with frequency is much faster than that of the imaginary part. This is because the loop becomes electrically larger at higher frequency, although it is still an electrically small loop antenna at the frequency range (50–400 MHz) considered. Although the loop ohmic-loss resistance also increase with frequency, the ohmic-loss efficiency in free space increases from 0.12% at 50 MHz to 46.8% at 400 MHz. Regarding the human-body coupling effect, as expected, the radiation resistance of the y-oriented loop is enhanced by the body and, hence, the ohmic-loss efficiency increases from 0.67% at 50 MHz to 67% at 400 MHz. For the body-absorption efficiency, higher efficiency means less body-absorption rate of the radiated power. It is observed that the body-absorption efficiency (for the y-oriented loop) is more than 60% when higher than 280 MHz. The total radiation efficiency has the same trend which increases from 0.19% at 50 MHz to approximately 45% at 400 MHz. For receiving system analysis in wireless-communication environments, the noise temperature T_A of the antenna is calculated by assuming $T_b = 200$ K and $T_p = 300$ K [see (10)]. Since the ohmic-loss efficiency increases with frequency, the noise temperature of the loop proximate to the body decreases from approximately 300 to 232 K at a 50–400-MHz

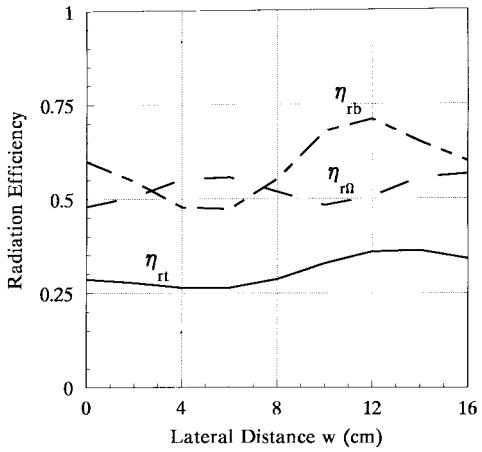

Fig. 5. Computed radiation efficiency of a y-oriented loop antenna proximate to a human body versus the lateral distance w from the center of the human abdomen. Loop radius $b = 1.7$ cm ($kb = 0.1$ at 280 MHz). Wire radius $a = 0.072$ cm (Hallen factor $2\ln(2\pi b/a) = 10$).

range. It is also noted that compared with the loop in free space, the noise temperature is approximately 30 K lower for the y-oriented loop proximate to the body when frequency is higher than 280 MHz. Table I also shows the maximum/minimum directive and power gains of the y-oriented loop in the H-plane at 280 MHz. For the E_θ pattern, although maximum directive gain is reduced from 1.52 dB in free space to -3.9 dB due to the body blocking and absorption effects, the maximum power gain is enhanced from -5.93 to -1.49 dB. This is contributed by the enhancement of the ohmic-loss efficiency by the body. The highly increasing of the minimum directive gain (from -100 dB to -9 dB) and power gain (from -100 dB to -14.47 dB) when proximate to the body also indicates the positive effect of the human body.

IV. Conclusion

Analysis and numerical computation of EM coupling between a circular loop antenna with different orientations and a full-scale human-body model from 50 to 400 MHz have been performed. The body has the highest absorption rate of the radiated power from the x-oriented loop antenna. Hence, the x-oriented loop may be suitable for the hyperthermia-applicator application to achieve efficient power deposition. The y- and z-oriented loop antennas are suitable for personal wireless-communication applications by considering the radiation efficiency and power patterns. Numerical results for the antenna input impedance, radiation patterns/polarization level, radiation efficiency, and power gain are important for the applications of different aspects.

References

[1] J. Toftgard, S. N. Hornsleth, and J. B. Andersen, "Effects on portable antennas of the presence of a person," *IEEE Trans. Antennas Propagat.*, vol. 41, pp. 739–746, June 1993.

[2] H.-R. Chuang, "Human operator coupling effects on radiation characteristics of a portable communication dipole antenna," *IEEE Antennas Propagat.*, vol. 20, pp. 556–560, Apr. 1994.

[3] M. A. Jensen and Y. Rahmat-Samii, "EM Interaction of handset antennas and a human in personal communications," *Proc. IEEE*, vol. 83, pp. 1–17, Jan. 1995.

[4] K. Fujimoto and J. R. James, *Mobile Antenna Systems Handbook*. Norwood, MA: Artech House, 1996, ch. 4.

[5] K. Ito, I. Ida, and M. Wu, "Body effect on characteristics of small loop antenna in pager systems" in *IEEE AP-S Int. Symp. Dig.*, vol. 2, Chicago, IL, July 1992, pp. 1081–1084.

[6] J. S. Colburn and Y. Rahmat-Samii, "Electromagnetic scattering and radiation involving dielectric objects," *J. Electromag. Waves Applicat.*, vol. 9, no. 10, pp. 1249–1277, 1995.

[7] H.-R. Chuang and W.-T. Chen, "Numerical modeling of EM coupling between a loop antenna and a 3-D lossy body object," in *Int. Symp. EMC*, Rome, Italy, Sept. 1996, pp. 204–209.

[8] J. Van Bladel, "Some remarks on Green's dyadic for infinite space," *IRE Trans. Antennas Propagat.*, vol. AP-9, pp. 563–566, 1961.

[9] D. E. Livesay and K. M. Chen, "Electromagnetic fields induced inside arbitrarily shaped biological bodies," *IEEE Trans. Microwave Theory Tech.*, vol. MTT-22, pp. 1273–1280, Dec. 1974.

[10] K. M. Chen, "A simple physical picture of tensor Green's function in source region," *Proc. IEEE*, vol. 65, pp. 1202–1204, Aug. 1977.

[11] D. P. Nyquist, K. M. Chen, and B. S. Guru, "Coupling between small thin-wire antennas and a biological body," *IEEE Trans. Antennas Propagat.*, vol. AP-25, pp. 863–866, Nov. 1977.

[12] A. D. Yaghjian, "Electric dyadic Green's functions in the source region," *Proc. IEEE*, vol. 68, pp. 248–263, Feb. 1980.

[13] K. Karimullah, K. M. Chen, and D. P. Nyquist, "Electromagnetic coupling between a thin-wire antenna and a neighboring biological body: Theory and experiment," *IEEE Trans. Microwave Theory Tech.*, vol. 28, pp. 1218–1225, Nov. 1980.

[14] J. D. Kraus, *Antennas*. New York: McGraw-Hill, 1988, ch. 6.

[15] C. C. Johnson and A. W. Guy, "Nonionizing electromagnetic wave effects in biological materials and systems," *Proc. IEEE*, vol. 60, pp. 692–718, June 1972.

New Tunable Phase Shifters Using Perturbed Dielectric Image Lines

Ming-yi Li and Kai Chang

***Abstract*—This paper presents new tunable phase shifters using perturbed dielectric image lines (DIL's). The propagation constant in the DIL was perturbed by a movable metal reflector plate installed in parallel with the ground plane of the DIL. The phase shift was thus controlled and adjusted by varying the perturbation spacing between the DIL and movable reflector plate at a given operating frequency. A rigorous hybrid-mode analysis was used for calculating the dispersion of propagation constants in the perturbed DIL, and then for designing tunable phase shifters. *Ka*-band tunable phase shifters have been designed, fabricated, and tested. Measurement results agree well with theoretical predictions. The device is especially useful for millimeter-wave applications where traditional phase shifters are lossy.**

***Index Terms*—Dielectric image lines, millimeter waves, tunable phase shifters.**

I. Introduction

Dielectric image lines (DIL's) have reduced losses compared to microstrip lines at millimeter-wave frequencies since most of the signal travels in the low-loss dielectric region [1]. This structure

Manuscript received July 17, 1997; revised May 5, 1998. This paper originally appeared in the September 1998 issue of this TRANSACTIONS and is being reprinted here with the correct graphics. This work was supported by the NASA Lewis Research Center and the Texas Higher Education Coordinating Board's Advanced Technology Program.

The authors are with the Department of Electrical Engineering, Texas A&M University, College Station, TX 77843-3128 USA.

Publisher Item Identifier S 0018-9480(98)06150-X.